

Comparison of Tooth Interior Fatigue Fracture Load Capacity to Standardized Gear Failure Modes

By Baydu C. Al, Dr. Rupesh Patel, and Dr. Paul Langlois

A comparison of tooth interior fatigue fracture load capacity with the predicted bending and pitting fatigue capacities, as calculated according to standards. Effects of several methods that can be used to mitigate TIFF risk are evaluated based on their performance, with respect to the other failure modes.

INTRODUCTION

Gears are case hardened to produce residual stresses at the surface — improving wear resistance, bending fatigue, and contact fatigue strength. These beneficial compressive stresses are balanced by tensile stresses within the core. This poses an increased risk of fatigue crack growth below the surface. Both tooth interior fatigue fracture (TIFF) and tooth flank fracture (TFF) — also known as tooth flank breakage (TFB) — describe a failure mode where a subsurface fatigue crack initiates close to case core boundary, at approximately mid-height of the tooth.

Previous research [1–8] has established that the direction in which the crack propagates and the appearance of the associated fracture is dependent on the flank loading (i.e. single-stage loading vs. idler usage). Although there does not appear to be total agreement in the literature, TIFF (failure with reverse loading) and TFF (failure with single flank loading) appear to have similar characteristics and crack initiation mechanisms. However, as shown in Figure 1, the final fracture shape is different, due to TIFF having near-symmetric total stresses along the tooth center line (with two possible initiation points per tooth). The location of the crack initiation distinguishes this failure mode from other fatigue failure modes.

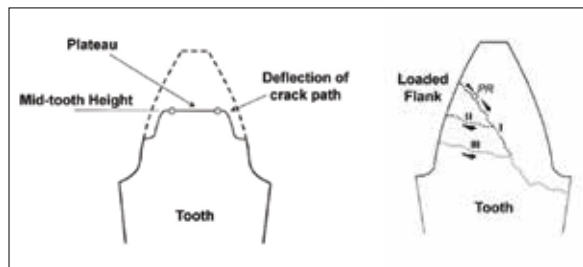


Figure 1 – Expected crack propagation paths for TIFF [1] (left) and TFF [4] (right).

TIFF and TFF failures can appear at loads below the allowable loading conditions for pitting and bending

fatigue failure modes based on internationally accepted calculation procedures (such as ISO 6336 [9] and AGMA 2101-D04 [11]). Therefore, understanding of TIFF and TFF failure modes is required at the design stage to avoid durability issues in the field. Previous research has shown the TIFF and TFF risk is dependent on the gear macro geometry, material, loading, and hardening properties.

As of the time of writing, there is no standardized method to assess the probability of this type of failure and the relative importance of the influencing factors. It is, however, worth noting TFF is an active topic within the ISO gearing committee, which is working on a draft standard, ISO/DTR 19042, for the calculation of tooth flank fracture performance.

BACKGROUND

In this manuscript, we give a brief summary of the calculation methods found in the literature for both TIFF and TFF, as recently discussed by Al and Langlois [12] and Al, et al. [13]. The proposed approaches for TIFF and TFF all have similar fundamental approaches consisting of four stages:

- Calculation of stress history.
- Calculation or specification of residual stresses.
- Calculation of equivalent stresses using some fatigue criterion.
- Comparison with some initiation thresholds based on field experience or experiments.

Each of the calculation methods described below differs in some of the details of the above steps. Further, the applicability of the methods depends on the assumptions made and the implementation details of each stage. Therefore, the implementation of each of these steps could be changed (different models or assumptions may be used), creating a number of permutations for engineers to choose from in order to achieve to a design requirement.

TOOTH INTERIOR FATIGUE FRACTURE CALCULATION METHODS

MackAldener [1–3] has shown that an analysis method based on 2D FEA can be used to analyze the risk of TIFF and determine optimum macro-geometry, material, and case-hardening properties. In this analysis, MackAldener used the gear load distribution analysis program LDP (Ohio State University Load Distribution Program) to calculate the total force on one tooth at different phases within the mesh cycle. The calculated force was then applied to a 2D

FE model of a single pair of teeth in contact as a torque after normalizing with the face width. A contact analysis was then run on the 2D FE model in order to calculate the stress history. MackAldener's papers show the evolution of the methodology used to estimate residual stresses and material properties. While MackAldener's early papers [1] described a methodology where transformation strain and material fatigue properties were assumed constant throughout the case, in his later papers these modeling assumptions were replaced with non-homogeneous profiles (see Sections 3.2 and 3.3).

Due to complexity of setting up and running MackAldener's FE-based method within a general FE package, MackAldener [2] also proposed a simpler semi-analytical method. This method was proposed for rapid calculation, design parameter studies, and optimization but with some compromise in the accuracy of the results. In the analysis of results presented in MackAldener [2], the crack-initiation risk factor result was seen to be over-predicted, as compared to MackAldener's FE-based method, by a maximum of 20 percent.

MackAldener used a factorial design to evaluate the effect of gear design parameters on TIFF risk and concluded that TIFF failure can be avoided if the slenderness ratio is reduced, tensile residual stresses are reduced, the gear is not used as an idler gear, and optimum case and core properties are used.

Al and Langlois [12] demonstrated a modification to the analysis of TIFF based on MackAldener's FE-based method, in which the loaded tooth contact analysis (LTCA) results from a specialized 3D elastic contact model, has been used to determine the load boundary conditions for analysis of TIFF. This replaces a computationally expensive, explicitly modeled FE contact analysis with simple load boundary conditions obtained by a separate specialized gear LTCA. This method has been validated against MackAldener's FE results.

TOOTH FLANK FRACTURE CALCULATION METHODS

The first model has been developed by FZG. This method has been published in Witzig [8], Tobie et al. [6], and Boiadjev et al. [7]. It relies on the calculation of the local stress history based on a shear stress intensity hypothesis of Hertz [14]. The method has significant empirical contributions and is limited in applicability due to the empirical nature of the equation used in calculating local material exposure. In the literature, this method has been presented for single flank loading only. It could, in theory be extended to consider double-flank loading (i.e. idler usage), but this is not trivial. As described by Witzig, this method requires Hertzian contact stresses as inputs, and these stresses can be calculated using a gear-load distribution program or via simplified analytical calculations such as those available in the standards. The method as published is also restricted to case-hardened gears, due to the assumptions related to the residual stress calculation. It should be noted that this method in its current form can

WHAT IS BARKHAUSEN NOISE?

Non-Destructive Evaluation for:

- ✓ Grinding burn detection
- ✓ Case depth measurement
- ✓ Heat treat defect detection
- ✓ Residual stress measurement



DOWNLOAD: Discover how this alternative method can improve your quality inspection process

stresstech.com/Barkhausen



Measure for success

Stresstech, a Nova Instruments company



underestimate the critical-fatigue stresses if resulting residual stresses within the core are not negligible, since these tensile stresses within the core are not taken into account. This assumption for the residual stresses is only valid when the core section is much larger when compared to the thickness of the case. This introduces limitations on applicability for slender teeth and extensive case hardening depths.

Ghribi and Octrue [5] proposed an alternative calculation method for TFF load capacity. This method is more generic than that of Witzig [8] and can be applied to both TFF and TIFF. The method proposes use of a multi-axial fatigue criterion and considers the importance of including tensile stresses in the core. The stress history is calculated using the Hertzian contact stress calculations of ISO/TR 15144-1 [16] micropitting load capacity calculation standard, together with a proposal of Johnson [17], to calculate stress at a depth inside the tooth. Method A of ISO/TR 15144-1 [16] is based on using the results of a 3D gear loaded tooth contact analysis; however, only Hertzian contact stresses calculated by the standard have been considered in the analysis. Addition of stresses due to bending has been mentioned as planned future work, as these stresses could have an impact on the calculated stress states.

Neither of these methodologies is based on finite element analysis (FEA), although they clearly could be adapted to do so. However, using general FE packages requires considerable time and computational power to set up and run analyses.

It is the author's opinion that the critical effect of material quality and inclusions is the key factor missing in the types of analyses presented. We would expect this could be addressed as a factor applied to, e.g., the material thresholds; however, significant field experience and further experimental studies are required to address this point.

Recently, Al, et al. [13] applied MackAldener's modified TIFF methodology [12] to TFF and showed a good correlation against the calculation method proposed by Witzig [8]. In contrast to methodologies presented by Witzig [8] and Ghribi and Octrue [5], this calculation method considered the whole stress tensor, including bending stresses. It should also be noted that failure thresholds obtained from Witzig's calculation differ from those obtained using the approach presented by Al, et al. [13], where a threshold close to 1 was found. Al, et al. [13] confirmed that ignoring tensile residual stresses within the core would cause under-

estimation of the critical fatigue stresses and showed the effect of tensile residual stresses increases with torque.

TIFF AND TFF RISK EVALUATION METHOD

This section reintroduces the methodology that was previously described and validated in our preliminary work (Al and Langlois [12], and Al, et al. [13]).

This methodology has been derived from MackAldener's finite element method, but the need for full FE tooth contact analysis has been removed by using loading condi-

tions calculated with a specialized loaded tooth contact analysis. MackAldener also simplified his FE analysis in a later stage, not for calculation of crack initiation risk factor, but when investigating the crack propagation mechanism [18]. These methods remove the complexity of the contact analysis and therefore speed up the calculation while reducing the computational requirements.

Analysis of Stress History

The specialized loaded tooth contact analysis (LTCA) model combines an FE representation of bending and base rotation stiffness



Sourcing Made Simple



Trusted Gear Blank Supplier Since 1950

- ▶ Consistent Quality
- ▶ Broad Capability & Capacity
- ▶ Exceptional People
- ▶ On-time Delivery

ISO 9001 and TS 16949 registered. Presses up to 4000T and volumes up to 750K/year. Supported by in-house heat treat and an ISO 17025 metallurgical lab.

walkerforge.com | 414.223.2000



of the gear teeth and blank with a Hertzian contact formalism for the local contact stiffness [15]. This calculation includes the effect of extended tip contact where the effective contact ratio is increased under load due to tooth bending. This effect can be particularly important for slender tooth gears, which are also more at risk of TIFF.

This model is used to determine load boundary conditions at a selected number of time steps through the mesh cycle. At each time step, the load distribution between and across the teeth is calculated, and at each of the contact lines, load positions, load magnitudes, and Hertzian half widths are obtained.

A separate fine 2D mesh of the gear tooth is then built automatically using plane-strain elements. At each time step within the mesh cycle, the position and distribution of the load is determined from the results of the 3D tooth contact analysis and applied to the 2D FE mesh, using the average load position and Hertzian half width. In the results presented in Section 4, the finite element mesh was sized according to the Hertzian half width, and a refinement study was performed to check the convergence of the results.

Hardness Profile and Material Properties

The variation of the material properties within the case and core play an important role in TIFF. However, many assumptions have been made in previous analyses in this area. Since the analyzed gear is case hardened, the material properties are not constant throughout the tooth. The critical shear stress, and the fatigue sensitivity to normal stress, in the critical plane criterion, are also expected to vary with location. As with MackAldener, for our analysis we have assumed these properties vary in the same way as an assumed hardness profile.

Hardness profile definition used by MackAldener [3]

$$H(z) = H_{\text{surface}} \cdot g\left(\frac{z}{\bar{z}}\right) + H_{\text{core}} \cdot \left(1 - g\left(\frac{z}{\bar{z}}\right)\right)$$

$$g\left(\frac{z}{\bar{z}}\right) = 1 - 3 \cdot \left(\frac{z}{\bar{z}}\right)^2 + 2 \cdot \left(\frac{z}{\bar{z}}\right)^3$$

EQUATION 3.2.1

where, H_{surface} and H_{core} are the hardness at the surface and core, respectively, g is a function which determines the variation between the case and the core defined by MackAldener, z is the normal depth at the point considered and \bar{z} is the total case depth.

MackAldener's method relies on measurement of the total case depth, which is often neither measured nor known. Therefore, as an alternative, a hardness measurement at a defined effective case depth is used. In such cases, a different hardness profile may be used, i.e. Lang [19], which is, in fact, the hardness profile used by Witzig [8].

Hardness profile definition used by Lang [19] and adopted by Witzig [8]

$$H(z) = H_{\text{surface}} \cdot g\left(\frac{z}{\text{CHD}}\right) + H_{\text{core}} \cdot \left(1 - g\left(\frac{z}{\text{CHD}}\right)\right)$$

$$g\left(\frac{z}{\text{CHD}}\right) = 10^{-0.0381\left(\frac{z}{\text{CHD}}\right) - 0.2662\left(\frac{z}{\text{CHD}}\right)^2}$$

EQUATION 3.2.2

in which CHD is the effective case depth, where hardness drops below 550 HV.

Comparison of hardness profile definitions

Figure 2 shows a comparison of the hardness profile measurement

and curve fit proposed by MackAldener with other hardness profile models found in the literature. Unless otherwise stated, for this article, MackAldener's curve fit has been used. It is interesting to note the hardness profile model proposed by Thomas [21] has been found to give the best comparison against MackAldener's measurement, and that of Tobe et al. [22] is also close.

The method of Lang could lead to a difference in the predicted risk of TIFF and TFF, since fatigue properties and residual stresses are expected to differ near the case-core boundary. This is demonstrated and further discussed in the results section.

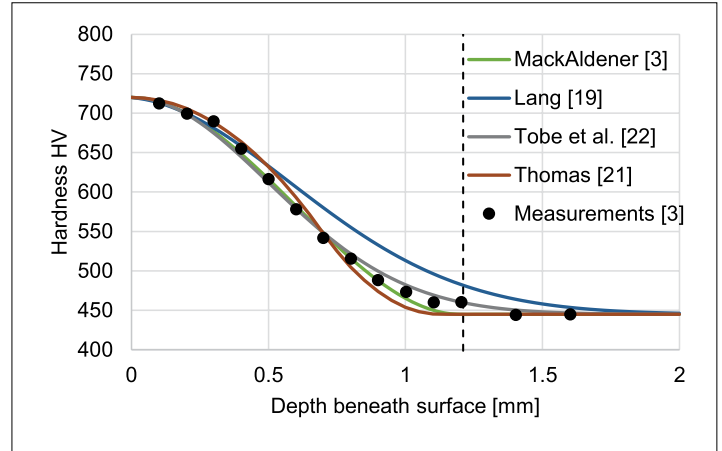


Figure 2 – Experimentally measured hardness profile and curve fits of MackAldener together with a number of empirical models available in the literature. The total case depth of 1.2 mm is marked by a dashed line. Effective case depth where hardness drops below 550HV is 0.68 mm (required for empirical models). See AI and Langlois for more information.

3.2.4 Determination of material properties required by multi-axial fatigue analysis

For the cases discussed in this manuscript, the material properties are assumed to vary continuously between case and core in the same manner as the hardness profile. This assumption is not required if variations of the material properties are known.

Critical shear stress

$$\sigma_{\text{crit}}(z) = \sigma_{\text{crit,surface}} \cdot g\left(\frac{z}{\bar{z}}\right) + \sigma_{\text{crit,core}} \cdot \left(1 - g\left(\frac{z}{\bar{z}}\right)\right)$$

Fatigue sensitivity to normal stress

$$a_{\text{cp}}(z) = a_{\text{cp,surface}} \cdot g\left(\frac{z}{\bar{z}}\right) + a_{\text{cp,core}} \cdot \left(1 - g\left(\frac{z}{\bar{z}}\right)\right)$$

3.3 Residual Stress Analysis

Residual stresses influence the stress states within the gear tooth. These stresses are not load dependent and are assumed to be constant over time. Residual stresses due to case hardening and shot peening are superimposed.

Residual stress calculation according to MackAldener [3]

Using the 2D mesh used to calculate the stress history due to flank loading, residual stresses are predicted by performing a separate FE analysis. The volume expansion in the surface layer due to the case-hardening process is modeled by applying a temperature profile to the FE model. The temperature profile applied is the same as the transformation strain profile when the coefficient of thermal expansion is set to 1. All side nodes are allowed to move only in the radial direction.

The transformation strain profile is isotropic and measured relative to the core. This profile has been presented as a piecewise polynomial with smooth connections by MackAldener [3].

$$\varepsilon_t(z) = \begin{cases} \varepsilon_1 + 4 \cdot (\varepsilon_2 - \varepsilon_1) \cdot \left(\left(\frac{z}{\bar{z}} \right) - \left(\frac{z}{\bar{z}} \right)^2 \right) & \text{if } 0 \leq z \leq \frac{\bar{z}}{2} \\ -4 \cdot \varepsilon_2 \cdot \left(1 - 6 \cdot \left(\frac{z}{\bar{z}} \right) + 9 \cdot \left(\frac{z}{\bar{z}} \right)^2 - 4 \cdot \left(\frac{z}{\bar{z}} \right)^3 \right) & \text{if } \frac{\bar{z}}{2} \leq z \leq \bar{z} \\ 0 & \text{if } \bar{z} \leq z \end{cases} \quad \text{EQUATION 3.3.1}$$

where:

- ε_1 is the transformation strain at the surface,
- ε_2 is the maximum transformation strain.

Residual stress analysis according to Lang [19] and modified by Witzig [8]

The calculation method proposed by Lang simply requires the heat-treatment type and depth from the surface to be known in order to calculate tangential residual stresses. As can be seen from the equations, only compressive residual stresses are calculated via this method. Note that $HV(z)$ in the equation refers to Lang's hardness profile as opposed to MackAldener's.

EQUATION 3.3.2

$$\sigma_{\text{residual}}(z) = \begin{cases} -1.25 \cdot (H(z) - H_{\text{core}}) & \text{if } H(z) - H_{\text{core}} \leq 300 \\ 0.2857 \cdot (H(z) - H_{\text{core}}) - 460 & \text{if } H(z) - H_{\text{core}} > 300 \end{cases}$$

This model has been used by both the TFF calculation methods proposed by Witzig [8] and Ghribi and Octrue [5]. The implementation described by Ghribi and Octrue can, however, also calculate tensile residual stresses by considering a force balance across the teeth. Note, this improvement on Lang's model has not been considered for this article.

Comparison of residual stress calculation methods

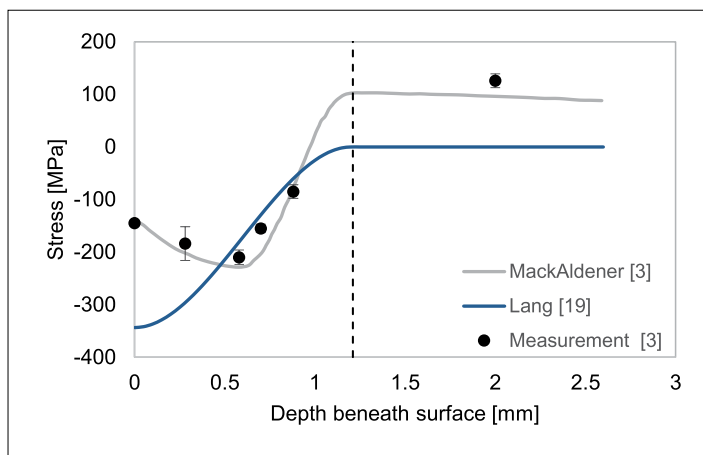


Figure 3 – Variation of residual stresses with increasing depth for the original gear set defined by MackAldener. The total case depth is marked by a dashed line. See Al and Langlois for more information. The residual stress profile, which is the result of the strain profile, has been used with $\varepsilon_1 = 0.000833$ and $\varepsilon_2 = 0.00114$ as determined by MackAldener [3].

Figure 3 shows the results presented by MackAldener for the variation of residual stresses with depth beneath the surface, both using the analysis method above and from measurements carried out by

MackAldener. Figure 3 further compares this residual stress profile with that proposed by Lang [19] and used by Witzig [8] in the investigation of TFF. Interestingly, the profiles differ quite notably. This may be due to a significant material dependency not considered, but the exact reason is unknown, and further understanding is required. It should be noted the resulting calculated residual stresses can change from one mesh position to another due to the variation in tooth thickness.

Final Stress State and Fatigue Crack Initiation Criterion

The effective stress state within the gear teeth during its load cycle is calculated — without calculating residual stresses at each step — by superimposing the calculated stress history states and the initially estimated residual stresses.

The Findley multi-axial fatigue criterion [20] is then used to analyze the stress history and assess the possibility of failure. Within our analysis, the Findley critical plane stress has been calculated for every 5 degrees of inclination at each node. The value of 5 degrees was chosen, instead of every 1 degree used by MackAldener [2], as results did not show a significant dependency on this value. This is confirmed by the cases presented in the results section of this manuscript where differences between using an inclination increment of 2.5 degrees over 5 degrees is less than 0.05 percent.

The Findley stress is calculated as: $\sigma_F = \tau_a + a_{cp} \times \sigma_{n,max}$ where τ_a is the shear stress amplitude, and $\sigma_{n,max}$ is the maximum normal stress. Variation of the material properties within the tooth is related to the hardness profile as described above.

The ratio between the maximum Findley critical plane stress and critical shear stress is a measure of the risk of crack initiation. This metric is called the crack initiation risk factor (CIRF).

Summary of author's method

Table 1 provides a brief summary of the methodology used throughout the rest of this manuscript.

Methodology described in this section has been derived from MackAldener's finite element method and has been previously validated in our preliminary work (Al and Langlois [12], and Al, et al. [13]).

DISCUSSION AND FUTURE WORK

This section covers three parts: The first investigates the effect of residual stress calculation methods on the crack initiation risk factor to establish if tensile residual stresses can be neglected; the second part aims to quantify the effect of possible design options for avoiding TFFF on the pitting and bending fatigue safety factors, and the last part investigates the torque ranges for each type of failure.

Effect of neglecting tensile residual stresses

MackAldener conducted a factorial design with five factors. In total, 32 designs have been considered by varying critical plane stress within the core (A), fatigue sensitivity to normal stress within the core (B), gear tooth geometry (C), total case depth (D), and torque on the pinion (E). For each of the factors, two levels, low and high, have been considered. Their values are presented in Table 2. Details of the gear tooth geometries are given in Table 3. For each of the designs, the CIRF throughout the tooth was calculated. Al and Langlois [12] previously used this study to validate the proposed methodology. The same factorial design experiment has been carried out using Lang [19] to specify residual stresses, where residual tensile stresses within the core are not considered.



**MANUFACTURING
TALK Radio**

The Voice of Manufacturing - Globally

**BREAKING MANUFACTURING
NEWS, TRENDS AND INSIGHT
LIVE EVERY TUESDAY AT 1PM EST
MFGTALKRADIO.COM
PODCAST ARCHIVED**

**SEAMLESS
ROLLED
RINGS**

& ALL-OPEN DIE FORGED PARTS



**ALL PARTS ROUGH
MACHINED
100% UT TESTED**

**108" MAX O.D.
6" MIN O.D.
UP TO 55,000 LBS**

ISO9001:2008 / AS9100C

**All Metals &
Forge Group**

STEELFORGE.COM

800.600.9290

973.276.5000

	Author's method	Author's method with Lang [19] for residual stresses
Stress History	Calculated using 2D FE analysis where the specialized LTCA model [15] has been utilized to obtain the load boundary conditions for the contact (section 3.1).	
Residual Stress State	Calculated using 2D FE where volume expansion specified as in MackAldener (section 3.3.1).	According to Lang [19] and used by Witzig [8]. Tensile stresses in the core are assumed negligible (section 3.3.2).
Equivalent Stresses	Calculated using Findley critical plane criterion [20]. Fatigue sensitivity to normal stress assumed to vary continuously in the same manner as the hardness profile. As in MackAldener (section 3.2.4 and section 3.4).	
Initiation Threshold	Calculated by dividing the maximum Findley plane stress by the permissible stress at a given point. Critical plane stress is assumed to vary continuously in the same manner as the hardness profile. As in MackAldener (section 3.2.4 and section 3.4).	

Table 1 – Summary of the author's calculation method

Factor	Description	Low level	Nominal level	High level
A	Critical plane stress within the core	359.85 MPa	479.8 MPa	559.75MPa
B	Fatigue sensitivity to normal stress within the core	0.28	0.37	0.46
C	Gear design	Slender	Original	Not-Slender
D	Total case depth	0.9 mm	1.2 mm	1.5 mm
E	Torque on the pinion	1238 Nm	1651 Nm	2064 Nm

Table 2 – Summary of factors used in the factorial design [2]

	Slender		Original		Not-slender	
	Pinion	Wheel	Pinion	Wheel	Pinion	Wheel
Modulus [mm]	2.34		3.06		3.75	
Pressure angle [°]	17.5		20		22.5	
Helix angle [°]	15					
Center distance [mm]	166.5					
Face width [mm]	43	35	43	35	43	35
Tip diameter [mm]	116.5	230.6	116.5	230.6	116.5	230.6
Profile shift coefficient	0.270	-0.669	0.65	0.250	0.6	0.895
Protuberance [mm]	0.06	0.095	0.06	0.06	0.06	0.06
Addendum for tool [mm]	4.85	3.9	4.35	4.35	4.35	4.8
Protuberance angle [°]	5.044	8.342	3.045	3.045	4.308	3.786
Tool edge radius [mm]	0.45	0.85	1.2	1.2	1.75	1.45

Table 3 – Gear data for the gear designs considered [2]

Figure 4 shows a comparison of the calculated maximum CIRF for all 32 designs. From Figure 4, it is clear there is a good overall correlation between CIRF calculated by the author's method and that calculated by MackAldener [2].

Figure 5 displays the average CIRF results for each factor at its low and high level together with the average for some interactions. It can be seen that good agreement exists for factors A, B, D, and E, and reasonable agreement for factor C.

Details regarding these comparisons are discussed in Al and Langlois [12]. The more interesting observation here comes from examining the cases where the author's method is used with Lang [19] for residual stresses. As can clearly be seen from Figure 4, this approach underestimates the maxi-

imum CIRF in all designs investigated. Furthermore, using Lang [19] for residual stresses changes the relationships and some interactions expected from the factors, seen in Figure 5. This change can be attributed to differences in the hardness profiles and/or neglected tensile residual stresses within the core.

Effect of Factors on Pitting and Bending Safety Factors

Factor (C) gear design and Factor (E) torque on the pinion are two parameters investigated in the factorial design, which would have a direct effect on pitting and bending fatigue calculations, according to ISO 6336 [9]. It has been assumed all gears have a flank tolerance class of 5 according to ISO 1328-1 [10] and material quality

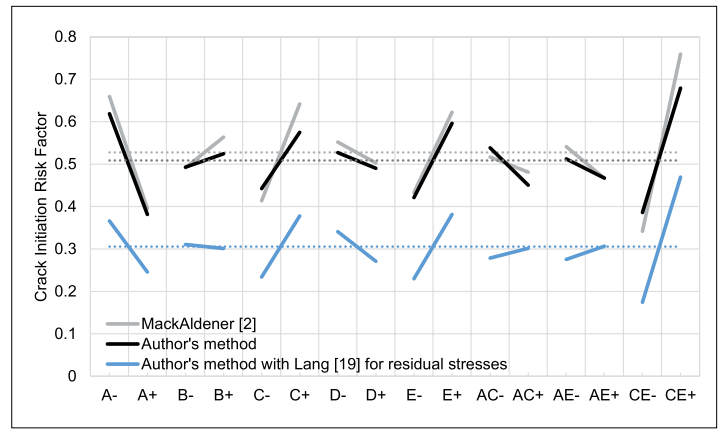
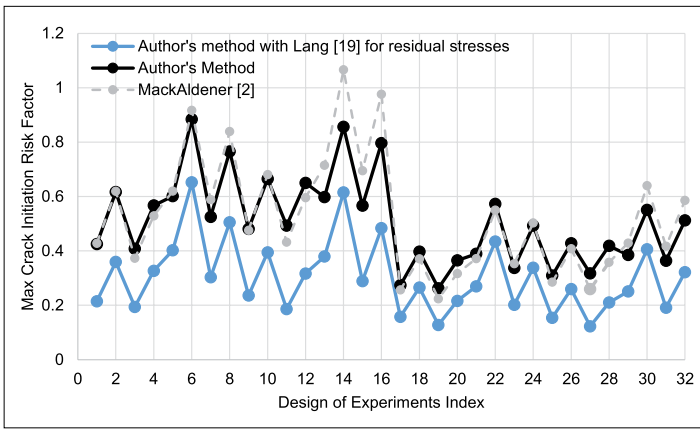


Figure 4 – Comparison of the calculated Maximum CIRF's using the author's method, author's method with Lang [19] for residual stresses, and MackAldener's finite element calculations. Index values have been determined by first sorting according to factor (A through E) then sorting the values of each factor in ascending order.

Figure 5 – Comparison of the effects of individual factors and their interactions on CIRF response for author's method, author's method with Lang [19] for residual stresses, and MackAldener's FE calculations. The dotted lines represent the mean response from each method.

grade of ME to get a representative theoretical comparison. It should be noted that other parameters could also potentially have an effect on the pitting and bending safety factors; however, internationally accepted calculation standards have assumptions based on the ISO material type selected.

Figure 6 shows how crack initiation risk factor, bending safety factor, and pitting safety factor vary with the change in the common factors that affect all three calculations. It should be noted that resistance to all three failure types can be improved by reducing the torque. For the cases investigated, a non-slender gear shows an improved safety against bending, however reduced safety for TIF and pitting. As

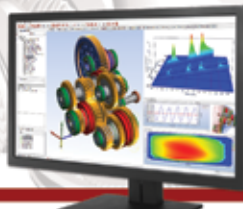
can be seen from Figure 6, both $1/\text{CIRF}$ and gear-bending fatigue are more sensitive to both geometry and loading compared to pitting.

Design domain for gears investigated by Witzig

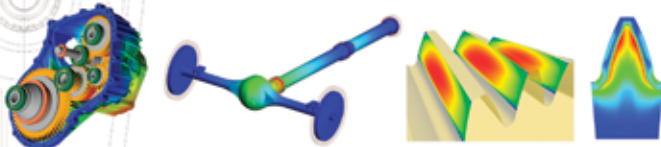
Details of gear tooth geometries and cutters specified by Witzig [8] are provided in Table 4. Gear set 67/69 with pressure angle 15° (details not provided here) could not be created from supplied tooth thickness and center distance information within Witzig's [8] thesis. For each design, the CIRF throughout the tooth was calculated, and trends have been compared to those obtained by Witzig [8]. Both of the gear-tooth geometries used within this article do not include any profile modifica-

MASTA

CAE solutions for the design, analysis and optimisation of complex transmission systems trusted by engineers worldwide




- Accurately and rapidly design and analyse transmission systems from scratch or troubleshoot existing designs
- Comprehensively understand the life of a mechanical part over the customer duty cycle
- Identify potential failure modes early in the development cycle
- Rapidly predict key performance characteristics at the design stage
- Easily explore changes in transmission layout, component selection and/or design, materials and manufacturing processes
- Perform full system simulations for any transmission or driveline configuration
- Incorporate manufacturing simulation at the design stage to reduce process development time & cost



Evaluate for free and discover more at masta.smartmt.com

Certified compatible with Windows 10



© 2017 Smart Manufacturing Technology Ltd.

A COMMON SENSE APPROACH IN THE MANUFACTURING OF WORLD CLASS GEARS



Raycar manufactures high quality smooth running gears offering competitive pricing and quick turn around.

- CNC GEAR BLANKING
- CNC GEAR SHAPING
- CNC GEAR HOBBING
- CNC GEAR GRINDING
- ANALYTICAL CHARTING EQUIPMENT
- UP TO 1000 PIECE LOT SIZES
- ISO 9001:2008



WE WANT THE OPPORTUNITY TO MAKE YOUR NEXT HIGH QUALITY GEAR SEND YOUR QUOTES TO:

Raycar Gear & Machine Co.
6125 11th Street
Rockford, IL 61109

Raycar
GEAR & MACHINE CO.

Phone: 815.874.3948
www.raycargear.com
sales@raycargear.com

tion other than a generous tip relief.

Based on the data provided by Witzig [8], transformation strains, surface and core critical stresses, and total case depth (see Table 2) for gears defined in Table 4 are estimated. Details of this analysis are provided in Al, et al. [13].

Figure 7 summarizes the results from Witzig [8] for spur gear set 67/69 (Figure 7a) and 40/41 (Figure 7b). It should be noted that the Y-axis on the right, for the maximum material exposure, is shifted to give comparable results (i.e. the critical value for the Findley criterion is expected to be 1 while for Witzig this critical value is 0.8).

The maximum crack initiation risk factors calculated using the author's method and author's method with Lang for residual stresses are extracted from Figure 7 and plotted together with pitting and bending fatigue safety factors in Figure 8. As can be seen in Figure 8, ISO Material Quality ML does not provide adequate resistance to either pitting or bending. As the material quality increases, the torque range over which TIFF failure could potentially occur, in comparison to pitting-and-bending failure, is seen to broaden. However, it should be noted that TIFF and TFF calculations, at present, do not take material quality into account. Using MackAldener's approach, this parameter could be included within the critical fatigue strength.

Figure 9 shows the effect of the flank tolerance class on pitting and bending fatigue safety factor. As can be seen from Figure 9, the increasing flank tolerance class reduces the safety factor at each load level and potentially reduces the torque interval over which TFF type of failure could occur. Also, it should be noted that TIFF and TFF calculations are not affected by any change to flank tolerance class (since friction between contacting surfaces has been assumed negligible, see Langlois et al. [15] for further details).

CONCLUSION

This study aimed to improve the existing understanding of Tooth Interior Fatigue Fracture load capacity and compare calculated load capacity to the allowable loading conditions for bending and pitting fatigue failure based on ISO 6336-1 [9] standard calculation procedures. Possible methods that could be used to mitigate TIFF risk have been presented, and the effect of these methods on the performance with respect to the other failure modes were quantified.

The key methodologies and conclusions from this manuscript are:

A parametric study initially conducted by

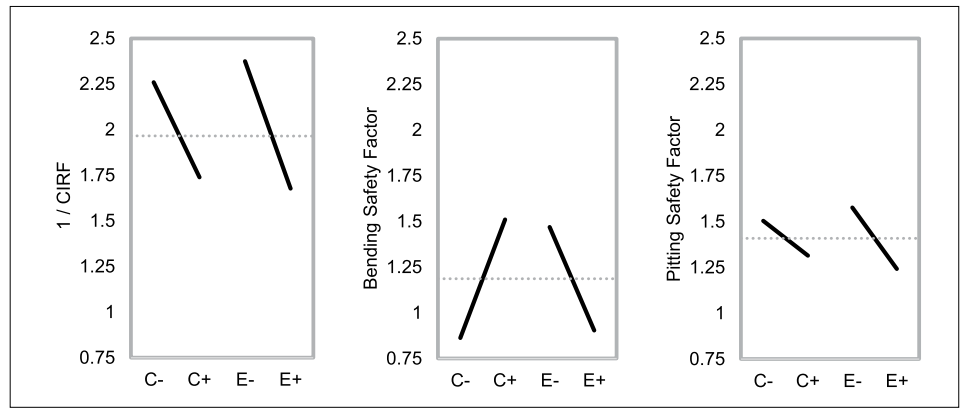


Figure 6 – Comparison of geometry and load effects on CIRF, Bending Safety Factor, and Pitting Safety Factor

Spur gear set designation	40/41		67/69	
	Pinion	Wheel	Pinion	Wheel
Number of teeth	40	41	67	69
Center distance [mm]	200		200	
Module [mm]	5		3	
Pressure angle [°]	20		20	
Profile shift coefficient	-0.23	-0.2456	-0.61	-0.6169
Tip diameter [mm]	205.6	210.2	201.2	207.16
Face width [mm]	18	18	18	18
Number of teeth measured for chordal span	5	5	7	6
Average chordal span measured [mm]	68.287	68.304	59.02	50.237
Assumed finish stock [mm]	0.04	0.04	0.04	0.04
Normal thickness of the cutter [mm]	7.854		4.712	
Protuberance [mm]	0.2		0.15	
Protuberance height [mm]	2.853		1.383	
Addendum for cutter [mm]	7.4		4.71	
Dedendum for cutter [mm]	5.6		4.54	
Cutter tip edge radius [mm]	2		0.81	
Cutter fillet radius [mm]	1		0.6	
Core Hardness HV	405		410	
Surface Hardness HV	695		695	
Effective Case Depth, HV550 [mm]	0.69		0.5	
Assumed Flank Tolerance Class	5		5	
Assumed Material Grade	MQ		MQ	

Table 4 – Gear and cutter data for the designs considered by Witzig [8]

Spur gear set designation	40/41		67/69	
	Surface, ϵ_1	Mid-case, ϵ_2	Surface, ϵ_1	Mid-case, ϵ_2
Transformation strain	0.000609	0.001163	0.000618	0.00121
Estimated total case depth	1.38 mm		0.98 mm	
Critical stress at surface	235 MPa			
Critical stress in core	675 MPa			

Table 5 – Estimated transformation strains and total case depth for gears defined in Table 4, assuming stresses at the surface can be obtained using Lang [19]. As given by Al, et al. [13]

MackAldener [2] to investigate which parameters influence the risk of TIFF and used for validation in Al and Langlois [12], has been revisited to investigate neglecting tensile stresses within the core using Lang [19] to specify residual stresses. As a result of this assumption, it has been found that the expected relationships between the factors are modified.

The common variables (i.e. gear geometry and torque) used in the calculation of the crack initiation risk factor, pitting resistance, and bending resistance have been investigated to extract the overall effects on all three failure types.

It has been shown that the torque range across which TFF failure can be seen could be relatively small compared to the operating range.

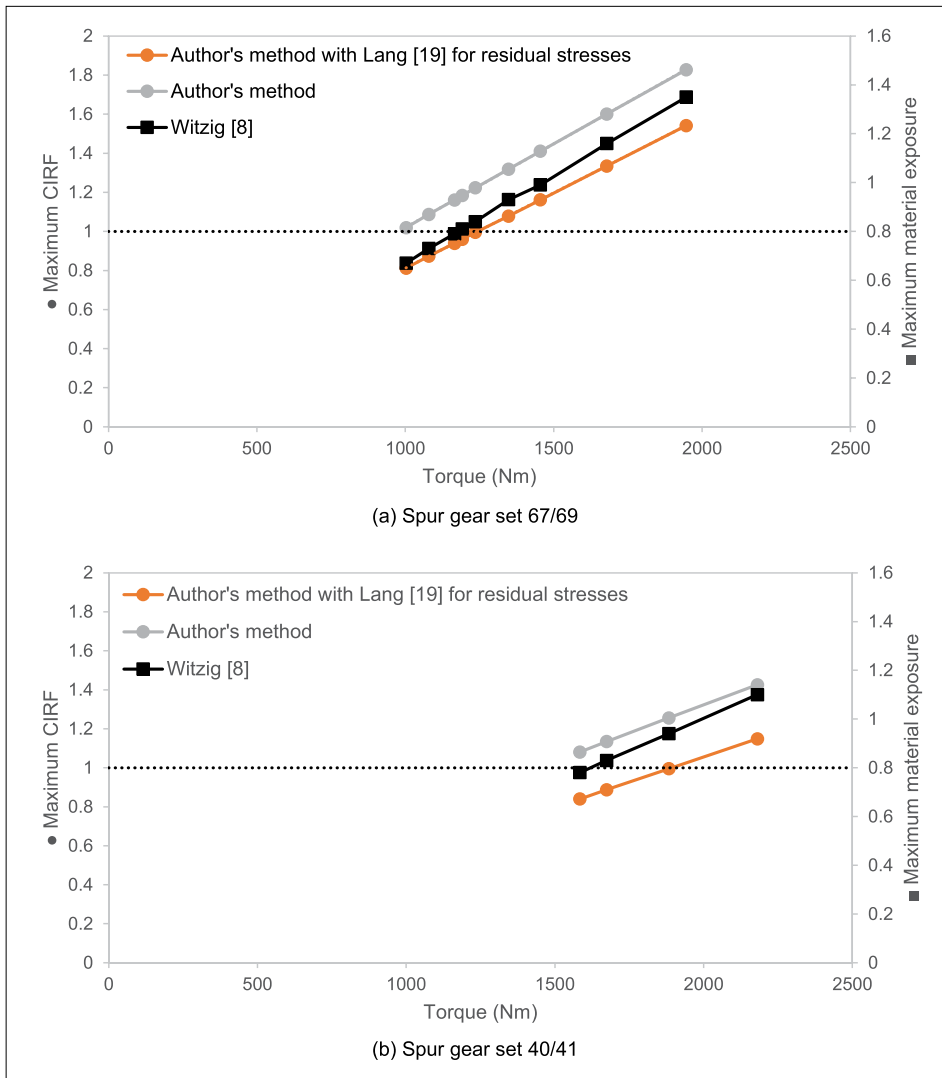


Figure 7 – Comparison of the calculated maximum CIRF's and Witzig's [8] method. It should be noted that the Y-axis of the maximum material exposure is shifted to give comparable results (i.e. critical value for Findley criterion is expected to be 1 while it is 0.8 for Witzig). The dotted line represents the expected critical value for the fatigue criterion used. As shown in Al, et al. [13]

Further investigations on the critical effect of material quality and inclusions are required to improve numerical calculation methods and standards. Further investigations into the design space to investigate a large set of gears comparing TIFF, pitting fatigue, and bending fatigue also is planned. 📄

BIBLIOGRAPHY

- MackAldener, M. and Olsson, M. (2000) Interior Fatigue Fracture of Gear Teeth, *Fatigue & Fracture of Engineering Materials & Structures*, 23 (4), pp. 283–292.
- MackAldener, M. and Olsson, M. (2000) Design Against Tooth Interior Fatigue Fracture, *Gear Technology*, Nov/Dec 2000, pp.18–24.
- MackAldener, M. and Olsson, M. (2001) Tooth Interior Fatigue Fracture, *International Journal of Fatigue*, 23, pp. 329–340.
- Bauer, E. and Bohl, A. (2011) Flank Breakage on Gears for Energy Systems, VDI International Conference on Gears, October 2010. Also *Gear Technology*, November/December 2011.
- Ghribi, D. and Octrue, M. (2014) Some theoretical and simulation results on the study of the tooth flank breakage in cylindrical gears, *International Gear Conference*, Lyon, France, 26–28 August 2014.
- Tobie, T.; Höhn, B. R. and Stahl, K. (2013) Tooth Flank Breakage — Influences on Subsurface Initiated Fatigue Failures of Case Hardened Gears. *Proceedings of the ASME 2013 Power Transmission and Gearing Conference*, Portland, OR, 4–7 August 2014.
- Boiadjiev, I.; Witzig, J.; Tobie, T. and Stahl, K. (2014) Tooth flank fracture – basic principles and calculation model



REBUILT Bryant and Technica Center Hole Grinders

- Standard & Extended Length Models
- Work Rotation & Steady Rest Attachments Available.
- All Machines Rebuilt and Guaranteed to New Tolerances.



Scan for Spec Sheet

HOFF MACHINERY
INCORPORATED

1325 Quincy St. NE
Minneapolis, MN 55413
Tel: 612.521.5700
Fax: 612.521.9358
www.hoffmachinery.com
webinfo@hoffmachinery.com

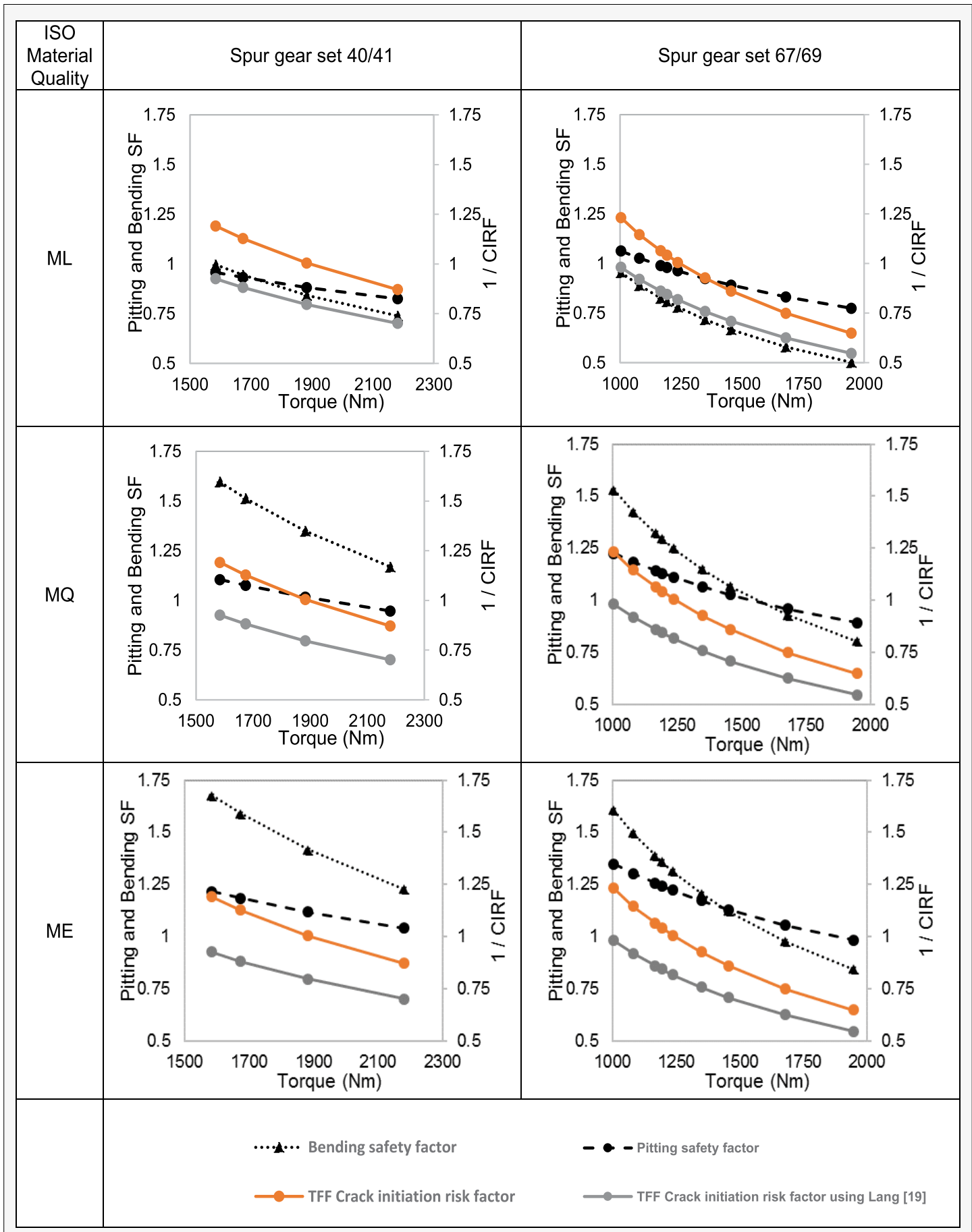


Figure 8 – Comparison of TFF load capacity with allowable loading conditions for bending and pitting fatigue failures based on standard calculation procedures (ISO 6336 [9]) for different material qualities. It should be noted that TFF does not consider material quality.

for a sub-surface initiated fatigue mode of case hardened gears, International Gear Conference, Lyon, France 26–28 August 2014. Also Gear Technology. August 2015.

8. Witzig, J. (2012) Flankenbruch Eine Grenze der Zahnradtragfähigkeit in der Werkstofftiefe. PhD Thesis, Technical University of Munich.
9. BS ISO 6336-1: 2006 Calculation of load capacity of spur and helical gears — Part 1: Basic Principles, Introduction, and General Influence Factors.
10. BS ISO 1328-1:2013 Cylindrical gears — ISO system of flank tolerance classification — Part 1: Definitions and allowable values of deviations relevant to flanks of gear teeth.
11. ANSI/AGMA 2101-D04 (2004), Fundamental Rating Factors and Calculation Methods for Involute Spur and Helical Gear Teeth.
12. Al, B. and Langlois, P. (2015) Analysis of Tooth Interior Fatigue Fracture Using Boundary Conditions from an Efficient and Accurate Loaded Tooth Contact Analysis, British Gears Association (BGA) Gears 2015 Technical Awareness Seminar, 12th of November 2015, Nottingham, U.K. Also Gear Solutions February 2016.
13. Al, B., Patel, R. and Langlois, P. (2016) Finite Element Analysis of Tooth Flank Fracture Using Boundary Conditions From LTCA. CTI Symposium USA, Novi, MI, 11–12 May 2016.
14. Hertter, T. (2003) Rechnerischer Festigkeitsnachweis der Ermüdungstragfähigkeit vergüteter und einsatzgehärteter Zahnräder. PhD Thesis, Technical University of Munich.
15. Langlois, P., Al, B., Harris, O. (2016) Hybrid Hertzian and FE-Based Helical Gear-Loaded Tooth Contact Analysis and Comparison with FE, Gear Technology, July 2016, pp. 54–63.
16. BS ISO/TR 15144-1:2014 Calculation of micropitting load capacity of cylindrical spur and helical gears — Part 1: Introduction and basic principles.
17. Johnson, K. L. (1985) Contact mechanics, Cambridge University Press. Oxford, U.K.

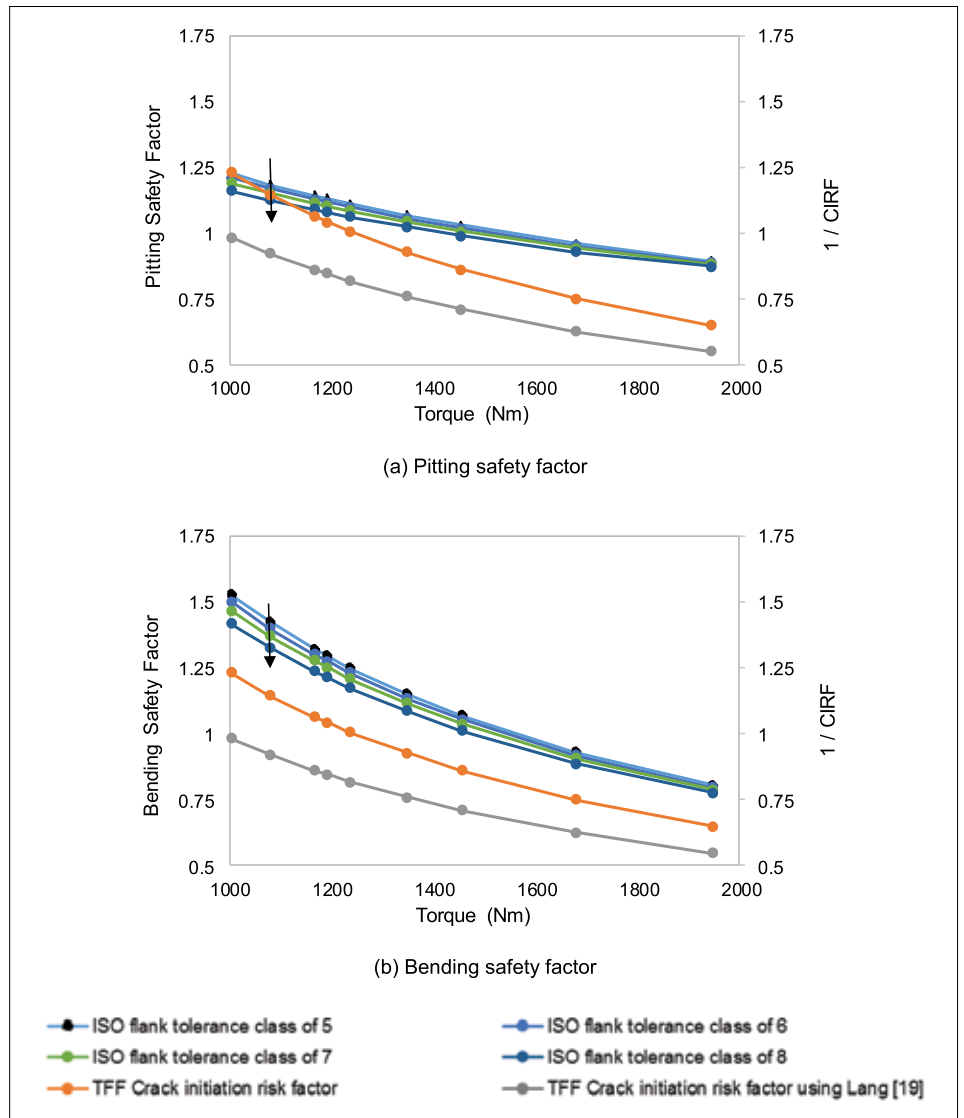


Figure 9 – Effect of increasing flank tolerance class (marked). It should be noted that TFF calculation does not consider flank tolerance class for spur gear set 67/69.

18. MackAldener, M. and Olsson, M. (2002) Analysis of Crack Propagation during Tooth Interior Fatigue Fracture, Engineering Fracture Mechanics, 69, pp. 2147–2162.
19. Lang, O. R. (1979) The dimensioning of complex steel members in the range of endurance strength and fatigue life, Zeitschrift fuer Werkstofftechnik, Vol. 10, p.24–29.
20. Findley, W. N. (1959) A Theory for the Effect of Mean Stress on fatigue of met-

als under combined torsion and axial load or Bending. Journal of Engineering for Industry, pp. 301–306.

21. Thomas, J. (1997) Flankentragfähigkeit und Laufverhalten von hartfeinbearbeiteten Kegelnradern. PhD Thesis, Technical University of Munich, Germany.
22. Tobe, T.; Kato, M.; Inoe, K.; Takatsu, N. and Morita, I. (1986) Bending strength of carburized C42OH spur gear teeth. JSME, p. 273–280.

ABOUT THE AUTHORS: Baydu Al has been an analyst/software engineer at SMT since October 2014. He has worked as a researcher at Nottingham University in gas turbine and transmission systems and specialized in efficiency and oil management prior to SMT. Since joining SMT, he has been contributing to MASTA's Loaded Tooth Contact Analysis and analysis of Tooth Interior Fatigue Fracture.

Dr. Rupesh Patel has worked at SMT as a systems analyst/software developer since January 2016. During this time, he has been actively involved in research and development of functionality for the analysis of tooth interior fatigue fracture and for gear macro-geometry optimization. Prior to employment at SMT, Patel worked for several years as a postdoctoral researcher at the University of Nottingham, specializing in structural dynamics and focusing on energy harvesting from natural sources of vibration. He was also employed overseas in Japan in relation to this work and has published numerous scientific papers over his career.

Dr. Paul Langlois is the CAE products development department manager at SMT. Having worked for SMT for 10 years, he has extensive knowledge of transmission analysis methods and their software implementation. He manages the development of SMT's software products and was a main contributor to many aspects of the technical software development. Paul contributes to ISO standards development for gears as a member of the BSI MCE/005 committee.